

Low loss high index contrast nanoimprinted polysiloxane waveguides

Ting Han^{1*}, Steve Madden¹, Mathew Zhang¹, Robbie Charters² and Barry Luther-Davies¹

¹ Laser Physics Center, Australian National University, ACT 0200, Australia

² RPO Inc. Innovations Building, 124 Eggleston Road, Acton, ACT 0200, Australia

*Corresponding Author: tih111@rsphysse.anu.edu.au

Abstract: Nanoimprint lithography is gaining rapid acceptance in fields as diverse as microelectronics and microfluidics due to its simplicity high resolution and low cost. These properties are critically important for the fabrication of photonic devices, where cost is often the major inhibiting deployment factor for high volume applications. We report here on the use of nanoimprint technology to fabricate low loss broadband high index contrast waveguides in a Polysiloxane polymer system for the first time.

©2009 Optical Society of America

OCIS codes: (130.5460) Polymers; (160.5470) Polymer waveguides.

References

1. H. Ma, A. K.-Y. Jen, and L. R. Dalton, "Polymer-based optical waveguides: Materials, processing, and Devices," *Adv. Materials* **14**, 1339-1365 (2002).
2. R. Buestrich, F. Kahlenberg And M. Popall, P. Dannberg, R. Muller-Fiedler and O. Rosch, "ORMOCERs for Optical Interconnection Technology," *J. Sol-Gel Sci. and Tech.* **20**, 181-186 (2001).
3. M. Usui, M. Hikita, T. Watanabe, M. Amano, S. Sugawara, S. Hayashida, and S. Imamura, "Low-loss passive polymer optical waveguides with high environmental stability," *J. Lightwave Technol.* **14**, 2338-2343 (1996).
4. T. Watanabe, N. Ooba, S. Hayashida, T. Kurihara, and S. Imamura, "Polymeric Optical Waveguide Circuits Formed Using Silicone Resin," *J. Lightwave Technol.* **16**, 1049-1055 (1998).
5. T. Watanabe, Y. Inoue, A. Kaneko, N. Ooba, and T. Kurihara, "Polymeric arrayed-waveguide grating multiplexer with a wide tuning range," *Electron. Lett.* **33**, 1547-1548 (1997).
6. A. W. Norris, J. V. DeGroot, T. Ogawa, T. Watanabe, T. C. Kowalczyk, A. Baugher, and R. Blum, "High reliability of silicone materials for use as polymer waveguides," *Proc. SPIE* **5212**, 76-82 (2003).
7. e.g. see www.gemfire.com and T. C. Kowalczyk and R. Blum, "Polymer variable optical attenuator arrays: pathway from material platform to qualified telecom product," *Proc. SPIE* **5517**, 50-61 (2004).
8. R. Charters, Redfern Polymer Optics Pty. Ltd., (personal communication, 2007).
9. S. Madden, M. Zhang, B. Luther-Davies, and R. Charters, "Patterning of inorganic polymer glass waveguiding films by dry etching," *Proc. SPIE* **6801**, 680107-1:7 (2008).
10. Y. Xia, G. M. Whitesides, "Soft Lithography," *Annu. Rev. Mater. Sci.* **28**, 153-84 (1998).
11. D. Kim, W. Chin, S. Lee, S. Ahn, and K. Lee, "Tunable polymeric Bragg grating filter using nanoimprint technique", *Appl. Phys. Lett.* **88**, 071120-1:3 (2006).
12. L. A. Rogers, M. Meier, A. Dodabalapur, E. J. Laskowski, and M. A. Cappuzzo, "Distributed feedback ridge waveguide lasers fabricated by nanoscale printing and molding on nonplanar substrates," *Appl. Phys. Lett.* **74**, 3257-3259 (1999).
13. Y. Huang, G. T. Palocz, A. Yariv, C. Zhang, L. R. Dalton, "Fabrication and replication of polymer integrated optical devices using electron-beam lithography and soft lithography," *J. Phys. Chem.* **B 108**, 8606-8613 (2004).
14. G. T. Palocz, Y. Huang, A. Yariv, J. Luo and A. K. Y. Jen, "Replica-molded electro-optic polymer Mach-Zehnder modulator," *Appl. Phys. Lett.* **85**, 1662-1664 (2004).
15. S. Kopetz, D. K. Cai, E. Rabe, and A. Neyer, "PDMS-based optical waveguide layer for integration in electrical-optical circuit boards," *AEU-Int. J. Electron. Commun.* **61**, 163-167 (2007).
16. S. Kopetz, E. Rabe, W. J. Kang, and A. Neyer, "Polysiloxane optical waveguide layer integrated in printed circuit board," *Electron. Lett.* **40**, 668-669 (2004).
17. W. S. Kim, J. H. Lee, S. Y. Shin, B. S. Bae, and Y. C. Kim, "Fabrication of ridge waveguides by UV embossing and stamping of sol-gel hybrid materials," *IEEE Photon. Technol. Lett.* **16**, 1888-1890 (2004).
18. A. Neyer, S. Kopetz, E. Rabe, W. J. Kang, S. Tombrink, "Electrical-Optical Circuit Board using Polysiloxane Optical Waveguide Layer," *Electronic Components and Technology Conference*, 2005. Proceedings, 55th. 2005

19. M. Vogler, S. Wiedenberger, M. Muhlberger, I. Bergmair, T. Glinsner, H. Schmidt, E. Kley, and G. Grutzner, "Development of a novel, low-viscosity UV-curable polymer system for UV-nanoimprint lithography," *Microelectron. Eng.* **84**, 984-988 (2007).
 20. K. K. Lee, D. R. Lim, H. C. Luan, A. Agarwal, J. Foresi, and L. C. Kimerling, "Effect of size and roughness on light transmission in a Si/SiO₂ waveguide: Experiments and model," *Appl. Phys. Lett.* **77**, 1617-1619 (2000).
 21. P. K. Tien, "Light waves in thin films and integrated optics," *Appl. Opt.* **10**, 2395-9 (1971).
 22. R. A. Bellman, G. Bourdon, G. Alibert, A. Beguin, E. Guiot, L. B. Simpson, P. Lehuède, L. Guiziou, and E. LeGuen, "Ultralow Loss High Delta Silica Germania Planar Waveguides," *J. Electrochem. Soc.* **151**, G541-G547 (2004).
-

Introduction

Polymers have long been recognized as leading candidates for the fabrication of low cost integrated optical components. The low fabrication cost opportunity arises from the combination of inexpensive materials, simple & fast processing techniques on low capital cost equipment, and the high index contrasts available to make small compact devices. Using polymer materials it is, for example, possible to fabricate waveguide devices very quickly using only spin coating and UV cure/solvent develop processes for patterning [1-2]. However, despite this promise there has been no demonstration to date of high index contrast waveguides fabricated by this route in materials known to be capable of passing the Telcordia reliability test suite. One polymer system well established to meet this requirement is the Polysiloxane class of materials. There have been demonstrations of low loss waveguide devices with up to 0.6% index contrast made by either plasma etching or the UV cure/develop process [2-6], and commercial devices are on the market [7]. However the relatively low index contrast precludes bend radii below 1cm severely limited the compactness of fabricated devices. Additionally there are known problems in fabricating structures much smaller than about 5 μ m with the UV cure process in Polysiloxanes [8], leaving plasma etching as the only demonstrated route [9]. The plasma etching route, whilst simpler than that for a comparable silica waveguide structure, is capital, consumable, and time intensive compared to the UV cure method. Thus we sought a simpler method to realize smaller high index contrast devices.

UV-Cured Nanoimprint Lithography (UV-NIL) is a non-photolithographic strategy based on replica molding for micro-fabrication. It offers low cost, fast processing using relatively inexpensive tools, and is a high throughput process for patterning microstructures [10]. Previously UV-NIL has been applied to fabricate integrated optical devices, e.g. optical couplers, lasers, resonators and modulators [11-14] in acrylate or epoxy based materials. Such materials, whilst excellent for nanoimprinting, do not have the same level of demonstrated environmental stability as Polysiloxanes. Kopetz et al. used the groove-filling method to fabricate large core multimode Polysiloxane and Polymethylsiloxane (PDMS) waveguides [15, 16]; Kim [17] also demonstrated large core (35x45 μ m) waveguides fabricated using UV-NIL on Sol-gel siloxane based material. The formation of a residual layer around the waveguide core after imprint was observed to be a problem; common solutions are reactive ion etching and "doctor blading" [18, 19]. Additionally, the large size of these waveguides masks the effects of surface roughness [20,21] meaning that the viability of small telecommunications compatible waveguides fabricated by nanoimprint is unproven.

In this paper we demonstrate for the first time, low loss, small, high index contrast Polysiloxane waveguides fabricated using UV-NIL. Low loss buried channel waveguides with core cross sections of 2-4 microns width and 3 microns height and a 2% refractive index contrast were fabricated on bare silicon wafers with a simple and fast three step process using a 100mm diameter PDMS stamp. The waveguides were patterned using an innovative "minimum fluid displacement" method which eliminated the residual films often seen either side of rib like features such as the waveguide cores, and which also produced very good dimensional control of the core itself regardless of the uncured spun core layer thickness. Thus this process also offers good manufacturing process tolerances. Further, the technology holds the promise of patterning complete passive devices including waveguide gratings for example to yield low cost wavelength division multiplexing devices with no increase in

production complexity or cost. Potentially the process can be scaled to a roll to roll implementation to generate very low cost devices.

IPG Waveguide materials

Inorganic polymers and Polysiloxanes are highly suitable for optical applications and have been developed to a commercial stage by NTT (deuterated siloxanes), Fraunhofer Institute (OrmocerTM), RPO (Inorganic Polymer GlassesTM), etc. Inorganic polymer glasses (IPGTM) are a type of photocurable Polysiloxane which have passed the stringent Telcordia environmental reliability criteria, have low birefringence and low loss at telecommunication wavelengths, and a tunable refractive index to yield index contrasts up to ~5%. The IPGTM materials available to us from RPO Pty. Ltd. had refractive indices of 1.507 for B11 and 1.478 for B3 at 1550 nm giving a refractive index step of 0.029 between the core and cladding for an index contrast of 2%. The thermo-optic coefficients for (dn/dT) are -3×10^{-4} /°C, coefficient of thermal expansion is about 600×10^{-6} /°C, and the decomposition temperature is larger than 300 °C, which is high enough for almost all optical applications.

Process and waveguide design

One property of the available IPG formulation was the relatively high viscosity (>2000cps), meaning that it is very hard to spin a thin layer (< 2 μm) on a substrate. Thus molding a rib for the core using a simple “trench” mold without a substantial residual layer on either side of the core was considered to be difficult proposition. With this in mind, we developed an approach which minimized the amount of fluid displaced during the imprint process by imprinting only a pair of isolation trenches, one either side of the core. This has the benefit of minimizing the quantity of displaced fluid and also focusing all the applied stamp force down through a small area thereby ensuring there is no residual layer either side of the core. The other benefit is that the spun liquid film thickness can be greater than the final required core height providing a greater degree of process tolerance.

Waveguide modeling with the full vector complex generic Finite-Difference method as embodied in the C2V Olympios software identified that the optimum core size for a 2% index contrast was a waveguide core of 3x3μm. The resulting fundamental mode profile is shown in Fig. 1(a). This is the best confined mode attainable with this index contrast and also provides the optimal mode match (loss < 0.1 dB) to available high numerical aperture fibers such as Nufern UHNA-3 fiber which can itself be spliced with low loss to standard telecommunications fibers for pigtailed. The 2% index contrast is also sufficient to bend this waveguide design with a minimum bend radius of ~1mm [22] meaning compact waveguide circuits can be realized. Modeling of the radiation mode coupling loss into slab modes of the non-imprinted core layer region suggested that the cladding/isolation trench needed to be at least 7 μm wide as shown in Fig. 1(b). The final width selected was 10μm to allow a safety margin. Waveguides were spaced at 125 microns centers meaning the displaced fluid volume during imprint was <20%, which could easily be taken up in the flexible mold areas either side of the waveguide cores.

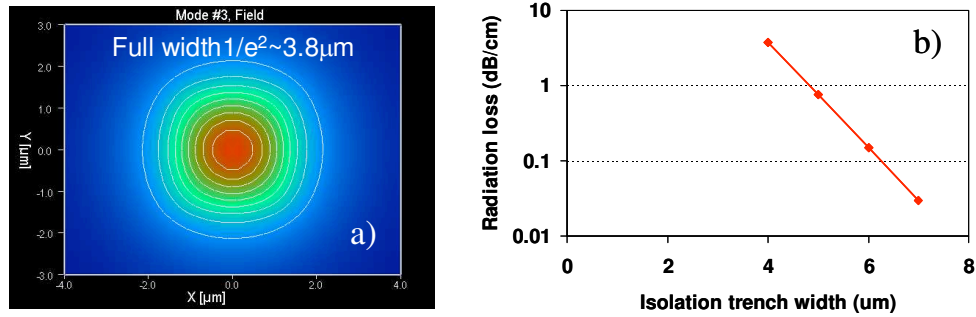


Fig. 1. (a). Fundamental mode field profile for $3 \times 3 \mu\text{m}$ waveguide with 2% index contrast. (b). Computed loss to radiation modes in unimprinted slab area vs isolation trench width.

Master and stamp fabrication

The waveguide master used for stamp fabrication was fabricated on a 4 inch thermally oxidized silicon wafer using standard processes. The desired structures were patterned using standard contact lithography and ICP-RIE dry etched $3 \mu\text{m}$ in depth into the $5 \mu\text{m}$ thermal oxide layer using trifluoromethane and Argon. To prevent the PDMS material sticking to the master a 50 nm Teflon like film was deposited on top of the master as a stamp release layer using ICP power only in the etcher with trifluoromethane gas feed. It should be noted that this route for master fabrication was chosen only to produce a durable master; a much lower cost and faster alternative better suited to commercial application would be a directly photolithographically defined master using SU-8 for example.

PDMS (Sylgard 184 from Dow Corning) was used as the soft stamp for UV-NIL and prepared by mixing the base material and curing agent at a weight ratio of 10:1. The mixed PDMS was then poured onto the master, which was located on a leveled and flat surface in a vacuum oven (surface tension forces were sufficient to prevent the PDMS from flowing off the wafer for the typical 2-3mm thick stamps prepared in this work). The material was degassed under vacuum and curing was performed at 65°C for 3 hours to minimize shrinkage. The stamp was then peeled off manually after cooling. Up to ten stamps were made from a single master with no apparent degradation of the master's anti-stick coating.

Waveguide fabrication

One of the most attractive advantages of UV-NIL is the simplicity of the process. The fabrication process for the imprinted waveguides involves just four short process steps:

1. Spin coating & curing $15 \mu\text{m}$ bottom cladding
2. Spin coating $3 \mu\text{m}$ IPGTM B11 core
3. Imprinting the core material
4. Spin coating and curing $15 \mu\text{m}$ top cladding

The imprint step was carried out using a home built tool in an open (clean room) atmosphere. Normally air bubbles trapped during the process would be a major limitation necessitating operation in vacuum. Therefore, a different approach was adopted as illustrated in Fig. 2.

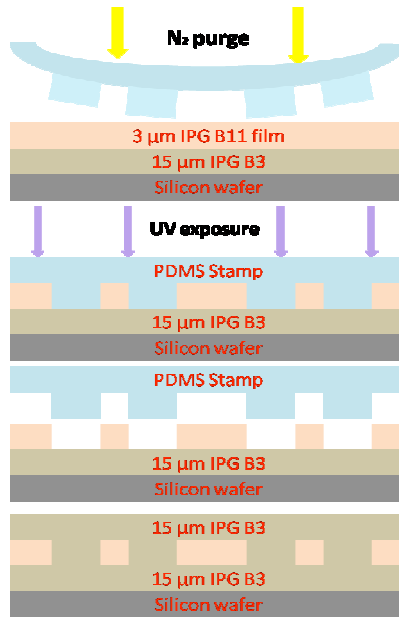


Fig. 2. Waveguide fabrication process (right)

Here a stamp holder comprising a 4 inch diameter ring with a vacuum groove and a transparent top cover was used to hold the stamp. Nitrogen purge was supplied to the internal space between the stamp and the glass plate allowing the stamp to be controllably bowed outwards via the applied pressure. The Silicon substrate with spin coated IPGTM film was mounted on a vacuum chuck with a motor driven vertical axis, and was driven up into contact with the stamp. The stamp holder was tilt adjusted such that the contact started in the center of the stamp and spread out radially as the substrate moved up. With this method, all air was expelled along the waveguide grooves and void free imprints were routinely attained. The core layer was then cured under UV light for 2 minutes and then the stamp was peeled off simply by driving the substrate downwards. The entire fabrication process from bare silicon to completed waveguide wafer took under an hour. Excellent surface morphologies and no residual layers were obtained in the imprinted waveguides as shown in Figs. 3(a)-3(c).

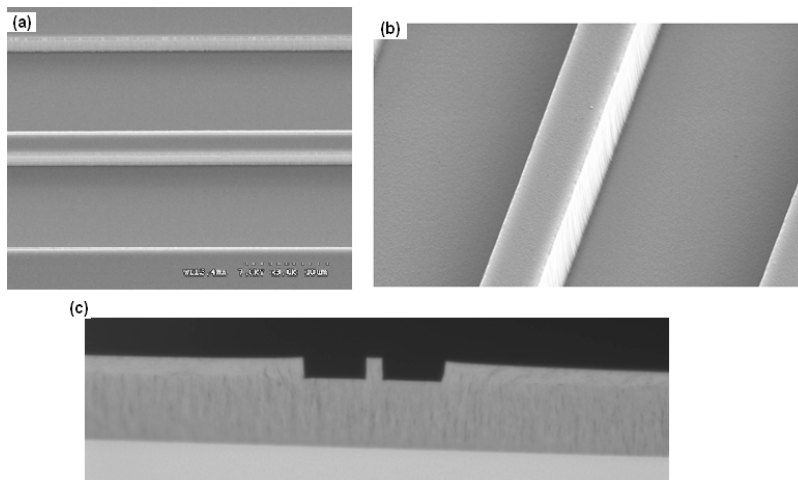


Fig. 3. (a). and (b). SEM images of imprinted waveguides. (c) .Cross sectional view of the imprinted waveguides under optical microscope.

A top cladding layer was then spun on and cured to complete the fabrication process. Waveguide chips were prepared from the finished wafer by hand cleaving with a diamond scribe.

Measurements and results

Coupling to the waveguides was accomplished using piezo controlled three axis stages at each end of the waveguide chip and Nufern UHNA-3 fibre. To index match the waveguides, drops of core IPG material without photo-initiator were used on the fibre ends to suppress the effects of reflections and facet imperfections, leaving misalignment or mode overlap as the only sources of coupling loss. As noted above, the expected mode overlap losses are small and the piezo stages and index matching made finding optimum alignment relatively simple. Light was injected from either a JDS/FITEL SWS 1501 tunable source at 1532nm or a white light source. The source was followed by a scanning polarization controller (Agilent 11896) to determine the polarization dependent loss (PDL), and signal detection was accomplished using a 150 μ m diameter SC-receptacled InGaAs detector with low PDL feeding a high accuracy six decade logarithmic amplifier (Analog Devices AD 757). The output from this was digitized with a 16 bit ADC card to make measurements. Figure 4 shows the results for cut back loss measurements at 1532nm, averaged over 5 waveguides of each width.

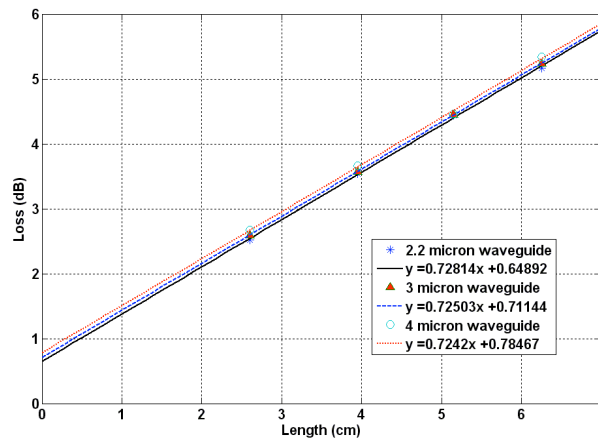


Fig. 4. Cutback results at 1532nm for various waveguide widths

The results at 1532nm show excellent linearity demonstrating the cut back measurement was valid, and for all waveguide dimensions show essentially the same loss (approx. 0.72dB/cm shown in Fig. 4 with a standard deviation on the loss for each width below 0.02dB/cm) suggesting scattering loss is not a contributor to the overall losses at 1532nm. The PDL of the waveguides was also measured and found to be essentially indistinguishable from the measurement system background. Note that the somewhat higher than expected coupling loss (~0.7dB measured vs ~0.1 dB predicted) was caused by an angle on the cleaved facets preventing the coupling fibers getting right up to the waveguide core. This resulted from difficulties in aligning the silicon wafer crystal plane to the waveguide stamp in the homebuilt imprint tool and is not a fundamental limitation.

The optical loss spectrum was obtained by fiber coupling a mercury arc lamp source into the waveguide and acquiring the spectrum at the waveguide output using an Agilent 86142B spectrum analyzer. The fiber coupled light source spectrum was then subtracted for normalization. Waveguide dimensions at 2.2 μ m, 3 μ m and 4 μ m were tested at 6.25cm and 2.6cm waveguide lengths respectively and the loss spectra at these two lengths subtracted and divided by the length difference to provide the actual propagation loss spectrum independent of wavelength dependent coupling losses, etc. Typical results are shown in Fig. 5(a) along

with the measured intrinsic material losses in a cured block of the material measured with a spectrophotometer.

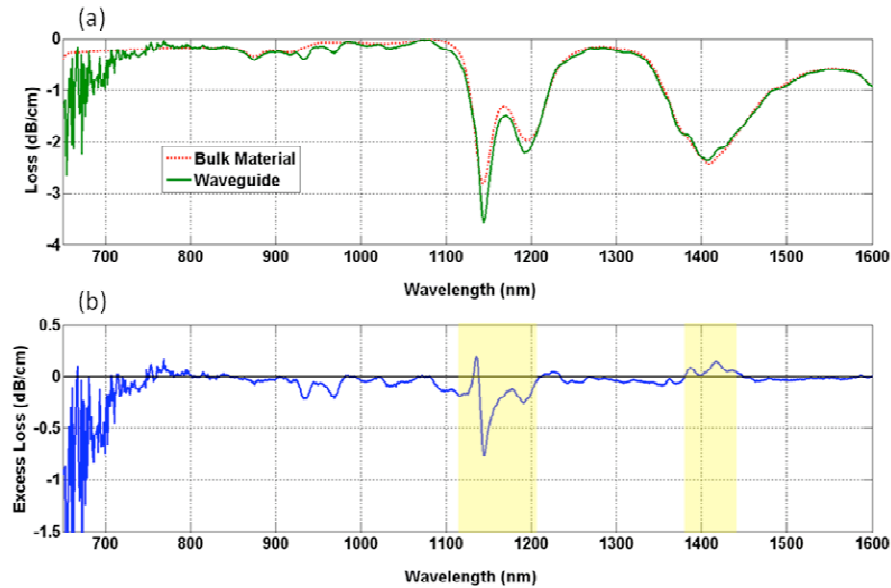


Fig. 5. (a). Optical loss spectrum of imprinted waveguide compared to the cured bulk material. (b) Excess loss introduced by waveguide (measurement regions highlighted by yellow boxes have reduced reliability due to differences in the resolutions and dynamic ranges of the measurement instruments for the fiber and bulk results).

The white light results gave the losses in the major transmission windows shown in Table 1. These results are essentially identical to the bulk material, with the exception of the 650nm figure (intrinsic loss here ~ 0.4 dB/cm). The discrepancy at 650nm may be due to a combination of modal effects between the waveguides and launch fibers and to waveguide sidewall scattering losses. These losses are certainly low enough for cost sensitive applications and can be further improved if necessary at higher material cost by fluorination or deuteration of the polymer materials [4]. Assuming the losses at wavelengths below 700nm are scattering related, these could also be further improved by depositing a thicker anti stick coating on the master as this has the effect of smoothing the sidewalls.

Table 1. Insertion losses at major transmission windows for imprinted waveguides

Wavelength (nm)	Loss (dB/cm)
650	2.0
850	0.22
1050	<0.1
1310	0.23
1550	0.58

Figure 5(b) shows the excess loss of the waveguide after subtracting off the measured intrinsic material losses and shows essentially zero excess loss from 750nm to 1600nm. There is no observable wavelength dependent loss in the transmission windows of interest indicating very low scattering loss and the high quality of the imprinting process.

The whole imprint process is also relatively insensitive to the spun thickness of the core material. Experimentally, we imprinted various wet film thicknesses from 2.7 μm to 3.8 μm , and there was no observable change in waveguide quality except the appearance of a thin residual layer as the film thickness rises above $\sim 3.5\mu\text{m}$ (300nm residual at 3.8 μm wet film thickness). The reproducibility of this process is critical in terms of mass production and was demonstrated by successive imprinting of 10 wafers using the same PDMS mold under the same imprint conditions. Comparing the 10th imprint to the 1st imprint, no noticeable changes for the waveguide dimensions or quality were visible under SEM observation.

Conclusion

In this paper, we demonstrated high quality Polysiloxane waveguides using UV-cured Nano-imprinting Lithography. With a core and cladding index contrast of 2%, waveguides with essentially no excess loss or PDL over a bandwidth spanning 750nm-1600nm were demonstrated. It has been demonstrated that this fabrication process is highly repeatable with excellent quality.

Acknowledgments

The support of the Australian Research Council through its Linkage grant and Federation Fellow programs is gratefully acknowledged, as is the financial support of RPO Inc.